

Analyst

Accepted Manuscript



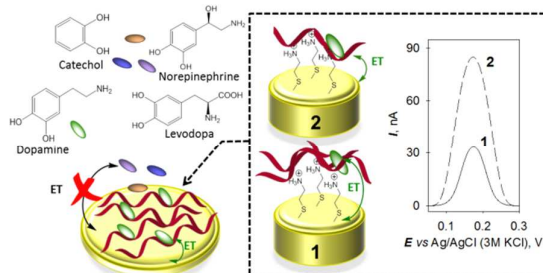
This is an *Accepted Manuscript*, which has been through the Royal Society of Chemistry peer review process and has been accepted for publication.

Accepted Manuscripts are published online shortly after acceptance, before technical editing, formatting and proof reading. Using this free service, authors can make their results available to the community, in citable form, before we publish the edited article. We will replace this *Accepted Manuscript* with the edited and formatted *Advance Article* as soon as it is available.

You can find more information about *Accepted Manuscripts* in the [Information for Authors](#).

Please note that technical editing may introduce minor changes to the text and/or graphics, which may alter content. The journal's standard [Terms & Conditions](#) and the [Ethical guidelines](#) still apply. In no event shall the Royal Society of Chemistry be held responsible for any errors or omissions in this *Accepted Manuscript* or any consequences arising from the use of any information it contains.

Graphical abstract



Electrochemical label-free aptasensor monitors physiological levels of dopamine with improved sensitivity when the aptamer surface coverage is optimized and with no interference from other catecholamines

Surface State of the Dopamine RNA Aptamer Affects Specific Recognition and Binding of Dopamine by the Aptamer-Modified Electrodes

Cite this: DOI: 10.1039/x0xx00000x

Isabel Álvarez-Martos^{a,b}, Rui Campos^{a,b} and Elena E. Ferapontova^{a,b*}

Received 00th January 2012,

Accepted 00th January 2012

DOI: 10.1039/x0xx00000x

www.rsc.org/

Specific monitoring of dopamine, in the presence of structurally related neurotransmitters, is critical for diagnosis, treatment and mechanistic understanding of a variety of human neuropathologies, and nevertheless the proper tools are scarce. Recently, an electrochemical aptasensor for specific analysis of dopamine, exploiting dopamine biorecognition by the RNA aptamer electrostatically adsorbed onto a cysteamine-modified electrode, has been reported (*Analytical Chemistry* 85 (2013) 121). However it was not clear which way dopamine biorecognition and binding by such aptamer layers proceed and if it can be improved. Here, we show that the aptamer surface state, in particular the aptamer surface density, in a bell-shaped manner affects the dopamine binding, being maximal for the 3.5 ± 0.3 pmol cm⁻² monolayer coverage of the aptamer molecules lying flat on the surface. Therewith, the aptamer affinity for dopamine increases one order of magnitude due to electrostatically regulated immobilization, with the aptamer-dopamine dissociation constant of 0.12 ± 0.01 μ M versus 1.6 ± 0.17 μ M shown in solution. Under optimal conditions, 0.1-2 μ M dopamine was specifically and 85.4 nA μ M⁻¹ cm⁻² sensitively detected, with no interference from structurally related catecholamines. The results allow improvement of the robustness of dopamine monitoring by aptamer-modified electrodes in biological systems, within the 0.01-1 μ M dopamine fluctuation range.

Introduction

Dopamine is an important neurotransmitter (NT) in the central nervous system that regulates movement, endocrine function, reward behavior, and memory processes.¹ A variety of human pathologies have been linked to alterations in neuronal release and uptake of dopamine, such as neuropsychiatric disorders (depression, schizophrenia, attention deficit hyperactivity disorder)², neurodegenerative diseases (Parkinson's disease),³ and drug addiction.^{4,5} As a result of its biological and medical significance, precise and selective *in vivo* analysis of dopamine at its 10 nM - 1 μ M levels characteristic of living systems⁶ is of great significance for clinical diagnosis and monitoring of treatment of the diseases and understanding mechanisms of their development.

Traditionally, detection of dopamine is performed *via* well-established "separation and detection" techniques.⁷ Although these methods provide high sensitivity of dopamine analysis, they have such drawbacks as (i) the requirement of sample pretreatment, (ii) poor spatial resolution, (iii) complexity of the

accompanying technical set-up, and (iv) long analysis times. With the aim of understanding the NT metabolism and their function *in vivo*, many efforts have been focused on developing invasive electrochemical sensors,⁸ which allow real-time detection and millisecond-range responses, can be easily miniaturized and are cost-effective. However, the selectivity of the electrochemical sensors for dopamine analysis may be compromised by the presence of other chemically-related neurotransmitting molecules with similar redox potentials such as catechol, norepinephrine, epinephrine, levodopa (L-DOPA) and some other⁹ and interference from other species with overlapping oxidation potentials such as ascorbic acid (AA) and uric acid (UA).^{10,11} To overcome AA and UA interferences the surface of the electrodes can be either electrochemically pretreated¹² or chemically modified with a wide range of materials, including self-assembled monolayers, metal nanoparticles and metal oxides, conducting polymers, graphene and its composites with nanoparticles, carbon nanotubes, nanowires, and permselective membranes,¹³ those modifications demonstrating improved selectivity and sensitivity of analysis in the presence of AA and UA.⁸ Despite all innovative technologies, the major problem of interference of other, structurally related NT with the selective analysis of dopamine has not been overcome.

Recently, we have reported an electrochemical RNA-aptamer based biosensor for specific analysis of dopamine in the presence of other NT.⁹ High specificity of ligand binding by

^a Interdisciplinary Nanoscience Center (iNANO) and ^b Danish National Research Foundation: Center for DNA Nanotechnology (CDNA), Aarhus University, Gustav Wieds Vej 1590-14, DK-8000 Aarhus C, Denmark

Corresponding author's e-mail address: elena.ferapontova@inano.au.dk

aptamers makes them excellent antibody-competitive biorecognition units for selective and sensitive analysis of a variety of analytes,^{14,15} including such small molecules of clinical interest as cocaine and theophylline.^{16, 17} In the particular case of dopamine, the aptamer-based biosensor allowed the clinically required sensitivity and selectivity of dopamine analysis in the presence of structurally related NT that were electrochemically active in the same potential window as dopamine itself.⁹ The aptamer was immobilized onto the positively charged cysteamine-modified electrode surface (Figure 1) and demonstrated a 0.1 μM dopamine detection limit and physiologically relevant linear range of 100 nM - 5 μM , where no interference from such structurally related NT as norepinephrine, epinephrine, L-DOPA, DOPAC, catechol, tyramine, and methyl dopamine was observed.

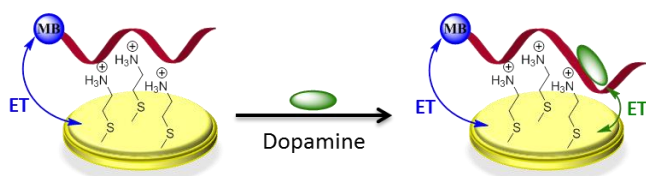


Figure 1. Schematic representation of the Methylene Blue (MB)-labeled aptamer immobilization and dopamine binding at the aptamer-modified electrode surface.

Therewith, it was not completely understood which way the aptamer immobilization at the electrode surface affected the aptamer-ligand biorecognition, we found a strong inconsistency between the aptamer and aptamer-bound dopamine surface coverages⁹ (discussed in more detail later). It was clear that the surface state and concentration of the aptamer should be critical for sensitive and selective binding of dopamine. Both factors are known to dramatically affect DNA-DNA interactions¹⁸ and electron transfer (ET) reactions between electrode-tethered DNA and redox indicators either covalently attached to DNA or present in solution,^{19, 20} and thus are to be implicated in dopamine-aptamer binding. In this context, electrochemical activity of dopamine as a ligand offered a unique opportunity to correlate binding properties of the aptamer (followed via dopamine electrochemistry) with the surface state of the aptamer (analysed from electrochemical responses of a redox label conjugated to the aptamer sequence, Figure 1).

Here, we studied the effect of the aptamer surface population and state on the dopamine binding ability, in order to correlate the activity of the aptamer, in the reaction of dopamine biorecognition and binding, with its surface state. We kept in mind that aptasensor properties are apparently pre-determined not by the overall number of the aptamer probe molecules at the electrode surface, but only by those able to capture the target analyte, dopamine. The probe surface density leading to the overcrowded interfacial environment may impede specific binding of dopamine by restricting the aptamer accessibility for dopamine molecules and capability of conformational changes concomitant the dopamine binding. Specific dopamine-binding ability of the aptamer that preconditions the overall sensor performance has been assessed by correlating signals from the methylene blue (MB)-labeled dopamine-specific RNA aptamer with those from the aptamer-bound dopamine, in order to establish conditions ensuring reliable analysis of the analyte.

Experimental section

Materials and reagents. Dopamine, norepinephrine, catechol, L-DOPA, ethanol (96%), Na_2HPO_4 , NaH_2PO_4 , NaCl, and cysteamine were purchased from Sigma-Aldrich (Germany). All chemicals were of analytical grade and used as received. The 57-mer Dopa_RNA aptamer for dopamine (5'-GUC UCU GUG UGC GCC AGA GAC AGU GGG GCA GAU AUG GGC CAG CAC AGA AUG AGG CCC-3')²¹ was synthesized by RiboTask (Denmark). The 5'-MB-labeled aptamer was prepared as previously described⁹ from 5'-amino-C₆-modified RNA aptamer obtained from RiboTask (Denmark). Water was purified by a Milli-Q reference A+ water purification system (18 M Ω , Millipore, Bedford, MA, USA). Stock solutions of catecholamines were daily prepared in 20 mM phosphate buffer solution containing 0.15 M NaCl (PBS), pH 7.4, and protected from light until analysis.

Instrumentation. Cyclic voltammetry (CV) and chronoamperometry (CA) measurements were performed in a conventional three-electrode electrochemical cell consisting of a gold working electrode (0.2 cm in diameter, CH Instruments, Austin, TX), an Ag/AgCl (3 M KCl) as the reference electrode (Metrohm, Denmark), and a platinum wire counter electrode, with a potentiostat AUTOLAB PGSTAT 30 (Eco Chemie B.V., Utrecht, The Netherlands) equipped with a NOVA 1.10 software. Working solutions were degassed with N_2 for at least 5 min prior data acquisition and kept under N_2 during the entire experiment. The reproducibility of the data was verified by measurements with at least four equivalently prepared electrodes. All measurements were performed at 22 ± 1 $^\circ\text{C}$.

Electrode modification. Prior modification, gold disk electrodes were cleaned in 0.5 M NaOH by potential cycling at 0.05 V s^{-1} , hand-polished to a mirror luster in 1 μm diamond and 0.1 μm alumina slurries (Struers, Denmark) on microcloth pads (Buehler, Germany), and ultrasonicated in ethanol/water solutions for 15 min. Afterwards, they were electrochemically polished in 1 M H_2SO_4 and 0.5 M $\text{H}_2\text{SO}_4/10$ mM KCl at 0.3 V s^{-1} . The electrode surface area was determined by integrating the reduction peak of gold surface oxide during the final scan in 0.1 M H_2SO_4 , assuming a theoretical value of 400 $\mu\text{C cm}^{-2}$ for a monolayer of chemisorbed oxygen on gold electrode,²² and was typically 0.084 ± 0.005 cm^2 . The electrodes were further water-rinsed and kept in ethanol for 30 min before modification. The electrodes were modified with cysteamine by placing a 10 μL drop of a 20 mM cysteamine solution onto the electrode surface (for 2 h under the lid). After a thorough rinse in PBS, the surface of the cysteamine-modified electrodes was exposed to 10 μL of a 10 μM aptamer solution. The aptasensor was stored at 4 $^\circ\text{C}$ between measurements. All solutions containing MB-aptamer/MB-aptamer modified electrodes were kept in dark.

Results and discussion

The surface coverage of the dopamine-specific RNA aptamer electrostatically adsorbed onto the cysteamine SAM-modified gold electrode, determined in our previous work by integration of the MB redox peaks in cyclic voltammograms (CVs) recorded with a MB-conjugated RNA aptamer, was 6.6 ± 0.5 pmol cm^{-2} (referred to the electrochemically active surface area).⁹ This surface coverage corresponds to a densely packed aptamer surface state, approaching the theoretical limiting surface coverage of vertically standing DNA duplexes of around 5.2×10^{12} molecules cm^{-2} (equivalent to 8.3 pmol cm^{-2}).²³ Obviously, the aptamer surface coverage of 6.6 pmol cm^{-2} is inconsistent with a monolayer of electrostatically adsorbed (and thus lying flat) ligand-active aptamer species. Along with

that, electroanalysis of dopamine binding to the unlabeled RNA aptamer immobilized at the electrode gave $1.86 \pm 0.12 \text{ pmol cm}^{-2}$ of bound dopamine (equivalent to the active aptamer surface coverage), and it is evident that such discrepancy can be due to the restricted dopamine binding ability of the aptamer in a densely populated aptamer monolayer or even a multilayer assembly. Adsorption of random coiled DNA on positively charged surfaces have also been reported to be accompanied by tangling and overlaying of DNA molecules in a multilayer film with a restricted ability for hybridization.^{24, 25}

Thus, the MB-labeled RNA aptamer was immobilized onto the positively charged cysteamine self-assembled monolayer (SAM)-modified gold electrode, and its dopamine-binding ability was studied as a function of the aptamer surface coverage, Γ_{RNA} , calculated by integrating the voltammetric signals stemming from either the MB redox transformation at -260 mV (the absolute aptamer surface coverage) or oxidation of the aptamer-bound dopamine at 200 mV (the dopamine-active aptamer surface coverage) (Figure 2). Both surface coverages were calculated according to the equation: $\Gamma_{\text{RNA}} = Q/nFA$, where Q is the charge associated with the redox peaks of either MB or dopamine, n is the number of electrons involved in the redox process, $n = 2$ for both reactions, F is Faraday's constant, and A is the electroactive surface area. The varying surface coverage of the aptamer was controlled by varying the aptamer immobilization time.

CV analysis of dopamine signals at the aptamer-modified electrodes demonstrated immediately a very different apparent sensitivity of analysis followed for different immobilization times, with the CV peak current intensities of dopamine oxidation being essentially lower in the case of longer aptamer immobilization times (Figure 2, data for 0.5 h (A) versus 2 h (B) immobilization are presented).

Therewith, the absolute aptamer surface coverage Γ_{RNA} increased with the increasing immobilization time (Figure 3A) and approached a saturation limit at $7.3 \pm 0.3 \text{ pmol cm}^{-2}$, for times exceeding 2 h. Along with that, storage of the aptamer-modified electrodes in the buffer solution for 1 h removed the

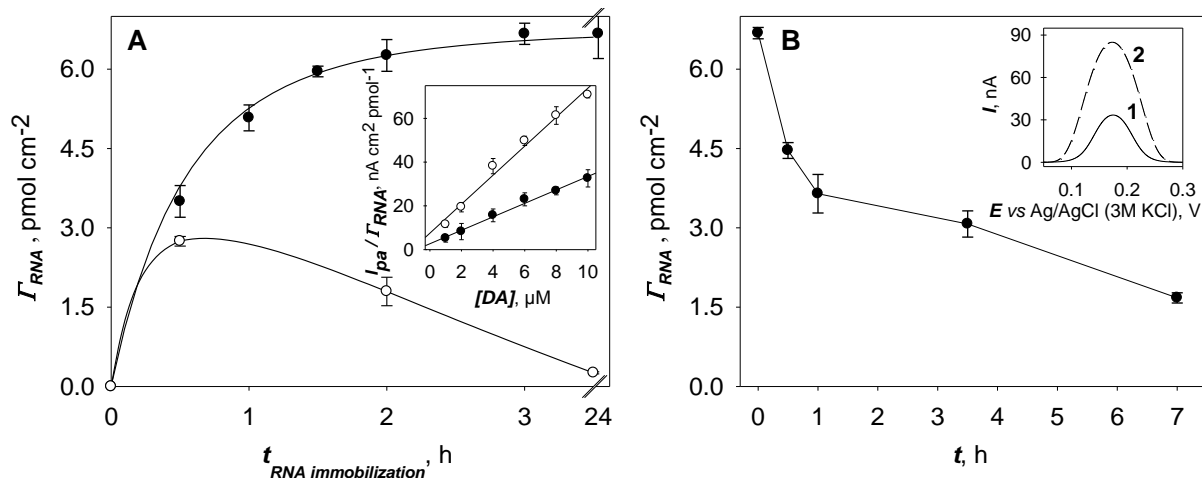


Figure 3. (A) Dependence of the aptamer surface coverage (Γ_{RNA}) on the aptamer immobilization time, Γ_{RNA} was estimated by integration of: (black circles) MB redox peaks (a solid line is Sigma Plot fitting to a hyperbolic increase function) and (empty circles) 2 μM dopamine oxidation peaks in CVs recorded with the MB-labeled aptamer/cysteamine-modified gold electrodes. Inset: Dopamine concentration dependence of the dopamine oxidation peak currents related to the total amount of the aptamer at the electrode surface for: (black circles) 2 h and (empty circles) 0.5 h of the aptamer immobilization. (B) Variation of the Γ_{RNA} (overnight immobilization, MB signals) on time, for the aptamer-modified electrodes stored in PBS between measurements. Inset: Background-corrected oxidation peaks of 2 μM dopamine, CVs recorded with the aptamer-modified electrode prepared by the overnight immobilization, (1) freshly prepared electrode and (2) after 1 h incubation in PBS. All data were derived from CVs recorded in PBS, potential scan rate 0.1 V s^{-1} . Surface coverage relates to the electrochemically active electrode surface area.

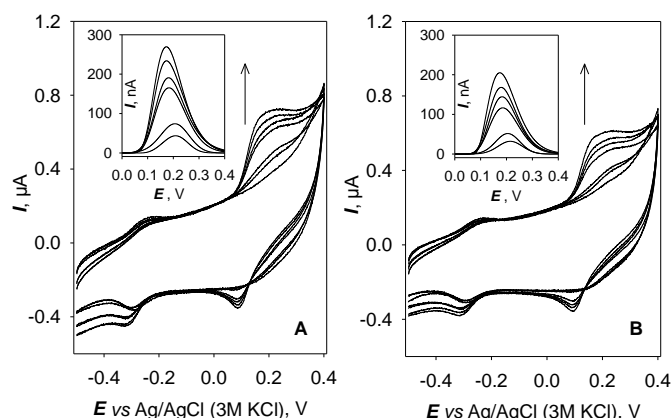


Figure 2. Representative CVs recorded with the aptamer-modified electrodes prepared by (A) 0.5 h and (B) 2 h aptamer immobilization, in PBS, pH 7.4, containing of 1, 2, 4, 6, 8 and 10 μM dopamine. Inset: background-corrected CV peaks of dopamine oxidation. The arrows designate the increasing dopamine concentration. Potential scan rate is 0.1 V s^{-1} , a polynomial baseline correction in the insets.

weakly adsorbed species with the desorption rate of $2.99 \text{ pmol cm}^{-2} \text{ h}^{-1}$, the surface coverage being reduced to $3.7 \pm 0.4 \text{ pmol cm}^{-2}$. After 1 h storage in PBS, the aptamer desorption slowed down to $0.33 \text{ pmol cm}^{-2} \text{ h}^{-1}$, and the Γ_{RNA} remained close to the 1 h values (RSD 12%) for at least 3 hours regardless of the time used for the aptamer immobilization (Figure 3B). For short immobilization times (0.5 h) the absolute aptamer surface coverage reached only $3.5 \pm 0.3 \text{ pmol cm}^{-2}$ and did not significantly change upon further storage. This variability in the surface adsorption behavior with immobilization time may be ascribed to the weaker adsorption and thus higher desorption rates of the long-time adsorbed aptamer, also due to the formation of the aptamer multilayers. Desorption of the aptamer molecules forming these multilayers from the electrode surface should finally result in the residual aptamer monolayer strongly attached to the positively charged cysteamine SAM.

In general, the anodic peak intensities (I_{pa}) stemming from the oxidation of the aptamer-bound dopamine (such as in Figure 3B, inset) should be proportional to the surface coverage of the dopamine-binding aptamer species according to the equation:²⁶

$$I_{pa} = (n^2 F^2 / 4RT) \Gamma_{RNA} A v \quad (1)$$

and reach their maximum values at the maximum surface coverage. However, the Γ_{RNA} dependence of the dopamine oxidation signals reflecting the dopamine binding ability of the immobilized aptamer had a bell-shaped form, with a maximum at the absolute aptamer surface coverage of $3.5 \pm 0.3 \text{ pmol cm}^{-2}$, and decreased with the increasing absolute Γ_{RNA} (Figure 3A, curve 2). This surface coverage (corresponds to 21×10^{11} molecules cm^{-2}) is indeed consistent with the RNA aptamer monolayer coverage with a footprint of the RNA aptamer molecule of $47.6 \pm 4.1 \text{ nm}^2$. If the RNA molecular diameter of 2 nm is assumed, derived as an extreme value from the DNA duplex diameter, then this footprint corresponds to the $0.42 \pm 0.04 \text{ nm}$ per base stretched RNA molecules adsorbed flat on the electrode surface. For comparison, the B-DNA duplex stretch per base pair may be estimated as 0.34 nm and that of RNA-A as 0.28 nm.²⁷

These results evidence that for the aptamer surface coverages exceeding the monolayer, the excessive aptamer adsorption achieved with longer immobilization times did not increase the response of the aptamer-modified electrode towards dopamine (that should result from the enhanced dopamine binding), but *vice versa* (Figure 3A, inset). This observation is in agreement with the concomitant loss of the aptamer affinity for dopamine molecules as the electrode surface becomes more and more crowded with the aptamer molecules that become more and more restricted in their dopamine-binding ability.

To further understand interactions underlying dopamine and aptamer binding we took into account the surface electrochemistry of dopamine oxidation at its concentrations below $2 \text{ }\mu\text{M}$ (a characteristic linear dependence of the oxidation peak currents on the potential scan rate). Under these conditions the dopamine binding to the aptamer followed the Langmuir isotherm behavior (at dopamine concentrations higher than $2 \text{ }\mu\text{M}$ there was a strong contribution from dopamine diffusing from the bulk solution to the electrode (Figure 4)). Keeping in mind a 1:1 stoichiometry of the RNA aptamer – dopamine complex, integration of the CV peaks corresponding to the $2e^-$ oxidation of the aptamer-bound dopamine allowed estimations of the surface population of the dopamine-active aptamer by fitting the data both to the Langmuir adsorption isotherm:²⁸

$$\Gamma = (\Gamma_{\max} K_b [\text{DA}] / (1 + K_b [\text{DA}])) \quad (2)$$

and the Scatchard model:²⁹

$$\Gamma = (\Gamma_{\max} [\text{DA}] / (K_d + [\text{DA}])) \quad (3)$$

Where Γ is the dopamine surface coverage, K_b reflects the ratio between the dopamine binding and dissociation rate constants at the aptamer-modified surface, K_d is the complex dissociation constant, and $[\text{DA}]$ is the dopamine concentration.

The Langmuir isotherms consistent with the dopamine binding to the aptamer sensing layers, prepared via 0.5 h and 2 h aptamer immobilization, level at $2.68 \pm 0.4 \text{ pmol cm}^{-2}$ (a monolayer of electrostatically adsorbed aptamer) and $1.86 \pm 0.12 \text{ pmol cm}^{-2}$ (the absolute aptamer surface coverage exceeds a monolayer),⁹ correspondingly, with the dopamine adsorption region (for 0.5 h) now being extended to $2 \text{ }\mu\text{M}$ due to the improved dopamine-binding ability of the aptamer (Figure 4). These results reflect

the improved dopamine-binding ability by the aptamer monolayer in comparison to the densely packed aptamer layers/multilayers exhibiting restricted binding ability of the aptamer.

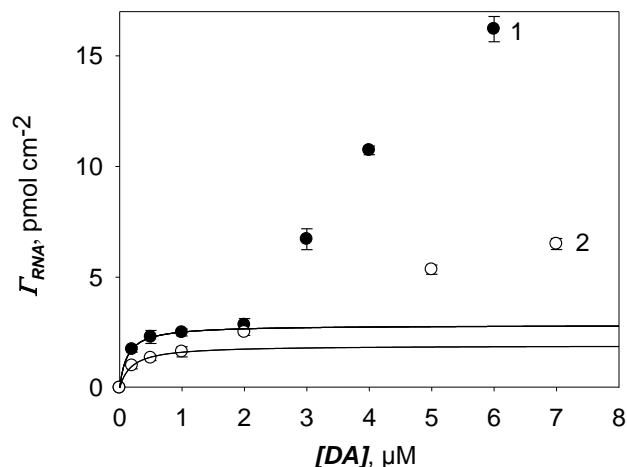


Figure 4. The aptamer surface coverage Γ_{RNA} estimated by integration of dopamine oxidation peaks recorded with the 0.5 h (1) and 2 h (2) aptamer/cysteamine/Au electrodes in solutions containing different concentrations of dopamine. Data on 2 h immobilization are derived from our previous work⁹ and included for comparison and discussion. The Γ_{RNA} relates to the electrochemically active electrode surface area. Solid lines are fitting to the Langmuir adsorption isotherm.

The binding affinity, K_b , of the RNA aptamer immobilized onto the cysteamine SAM for dopamine was $8.1 \pm 0.5 \text{ }\mu\text{M}^{-1}$ for 0.5 h aptamer immobilization time ($5.3 \pm 0.6 \text{ }\mu\text{M}^{-1}$ for 2 h immobilization), being in agreement with a higher specific affinity of the immobilized aptamer molecules towards dopamine and/or higher stability of the dopamine-aptamer complex. Importantly, the on-surface dissociation constant of the complex (K_d) of $0.12 \pm 0.01 \text{ }\mu\text{M}$ appeared to be order of magnitude smaller than that for the dopamine-aptamer complex in solution, estimated by equilibrium filtration to be $1.6 \pm 0.17 \text{ }\mu\text{M}$.²¹ The higher complex stability at the electrode surface can be correlated with the electrostatic regulation of the extent of ligand binding, in particular, with the electrostatic screening of the RNA sugar-phosphate backbone charges in the course of the RNA aptamer adsorption onto the positively charged cysteamine SAM. This allowed to minimize non-specific electrostatic interactions between the positively charged dopamine (and, actually, other, competitive catecholamine NTs) and negatively charged RNA and to improve specific binding of dopamine to the aptamer. Similar results, on a several orders of magnitude improvement of the aptamer affinity for its ligand achieved by electrostatic regulation, has been recently reported for the RNA aptamer specific for the urokinase plasminogen activator (UpA), in a 1 pM electrochemical aptamer assay for this protein cancer biomarker, which RNA-UpA complex stability in solution is characterized by the K_d in the nM range.³⁰

To directly correlate the dopamine binding ability with the surface coverage of the aptamer, the dopamine surface coverage (Γ_{DA} , equivalent to the number of dopamine-active aptamer molecules) was related to the absolute aptamer surface coverage (Table 1). As can be seen, the Γ_{DA}/Γ_{RNA} ratio decreased with increasing immobilization time, approaching unity at the lowest surface coverage. Therewith the affinity of the aptamer towards dopamine indeed correlates with the

surface population of the aptamer molecules: it was most pronounced at 3.5 pmol cm⁻² providing the most efficient biorecognition of dopamine by almost all aptamer molecules immobilized on the electrode surface. Specific sensitivity of dopamine analysis by the 0.5 h immobilized aptamer sensing layer, 79 A per mol of the aptamer and per M of dopamine, dropped down almost two-fold for the 2 h prepared sensor, then becoming 37 A mol⁻¹ M⁻¹ (see the slopes of the dependences in Figure 3A, inset), which is of direct analytical importance.

Table 1. Biorecognition activity of the surface immobilized aptamer expressed as a relationship between the dopamine and absolute aptamer surface coverages (Γ_{DA} and Γ_{RNA}).

Aptamer immobilization time, h	Γ_{RNA} , pmol cm ⁻²	Γ_{DA}/Γ_{RNA}
0.5	3.5 ± 0.3	0.78 ± 0.03
2	6.3 ± 0.3	0.27 ± 0.04
24	6.7 ± 0.5	0.039 ± 0.003

Thus, at immobilization times exceeding 0.5 h, the RNA aptamer molecules form either a tightly packed RNA monolayer or a multilayer, both being less active in dopamine biorecognition and binding as compared to the monolayer formed by the lying “flat” aptamer molecules not restricted in their dopamine binding ability. Despite the fact that a fraction of the aptamer molecules in the multilayer is weakly bound and can be easily removed either by the electrode storage in the blank buffer solution (Figure 3B inset) or during repetitive potential cycling (data not shown), it restricts the ability of other aptamer molecules to specifically recognize and bind dopamine. After removal of weakly bound species, the aptamer-modified electrodes become maximally active towards dopamine binding. In our previous work on specific analysis of dopamine by the aptamer-modified electrode,⁹ we produced the aptamer-modified electrodes with suppressed activity and current studies show the optimal conditions that allow the surface state of the aptamer molecules minimally restricted in its dopamine binding ability (Table 1, 0.5 h immobilization).

Finally, specific analysis of dopamine with the optimized aptamer-modified electrodes (0.5 h immobilization) was performed within the dopamine concentration range where aptamer-response is dictated by specific binding of dopamine to the surface-immobilized aptamer (below 2 μM, Figure 4, curve 2). A typical chronoamperometric response of the aptamer-modified gold electrodes to dopamine is presented in Figure 5. As can be seen in the inset, the specific current densities of dopamine oxidation, expressed as I/I_{RNA} , linearly increase with the increasing dopamine concentration in the range of 0.1–2 μM. The DA detection limit for the Γ_{RNA} of 3.5±0.3 pmol cm⁻² (the optimal aptamer surface coverage) was 0.1 μM, which is twice lower than 0.2 μM obtained for Γ_{RNA} = 6.3±0.3 pmol cm⁻² (the multilayer/densely-packed aptamer-modified electrodes). The specific (i.e. related to the absolute aptamer surface coverage) sensitivity of dopamine analysis by the aptamer monolayer electrodes was also higher than by the densely packed aptamer electrodes, 2.05 (nA μM⁻¹)/(pmol cm⁻²) versus 0.89 (nA μM⁻¹)/(pmol cm⁻²), correlating to the general sensitivity of analysis of 85.4 and 66.8 nA μM⁻¹ cm⁻², correspondingly (the latter lower value is consistent with a previously reported 62 nA μM⁻¹ cm⁻²).⁹ Such a two-fold improvement in the detection limit and specific sensitivity of the assay significantly improves the robustness of the dopamine analysis in the presence of other NTs (Figure 5, inset). No significant oxidation signal was detected when dopamine was

replaced by the competitive NT, norepinephrine, demonstrating both the ability of the aptasensor to specifically detect dopamine and improved discrimination between dopamine and structurally related neurotransmitters with similar redox potentials (Figure 5, inset, curve 3 versus curves 2 and 1). It is worth to mention that NT discrimination ability of the aptamer-modified electrodes is much improved compared to the aptamer’s ability in solution, which is insufficient for robust discrimination between, e.g., dopamine and norepinephrine (based on 100% and 58% ability of these molecules to elute the dopamine-agarose-bound aptamer).²¹

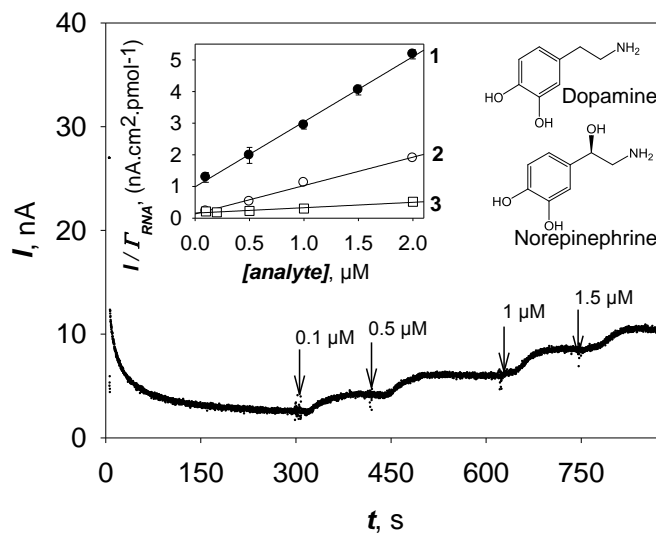


Figure 5. Representative chronoamperogram recorded in PBS, pH 7.4, with the 0.5 h immobilized aptamer-modified electrode upon successive additions of dopamine. Inset: Dependence of the specific currents of dopamine oxidation (expressed as I/I_{RNA}) on the dopamine concentration for (1) 0.5 and (2) 2 h aptamer-modified electrodes and (3) on the norepinephrine concentration, 0.5 h electrodes. Similar to (3) data were obtained for L-DOPA and catechol. $E_{detection}$: +0.185 V. The CA was performed in a 5 mL electrochemical cell with no stirring. The dopamine injections were done at a distance of ~3 cm from the electrode surface, so the ca. 20 s lag-period between the injection and response, due to the dopamine diffusion and aptamer binding, can be followed in the chronoamperogram.

The achieved sensitivity and specificity of the optimized aptamer system for dopamine analysis better satisfies the requirements for monitoring of *in vivo* fluctuations of dopamine during behavioral and pharmacological events, which generally occur in the range of 10 nM (a basal level) - 1 μM dopamine.⁶ Our results evidence that dopamine binding and the resulting biosensor performance is extremely sensitive to the surface state of the aptamer molecules and their population at the electrode surface. Denser surface states of the aptamer do not obligatory result in the best performance of the aptasensor, but *vice versa*, they result in the inhibited biosensor response and lower sensitivity for the analyte due to the restricted ligand binding ability. That may be applicable to other ligand-aptamer electrode systems in which electrochemically inactive ligands unfortunately do not allow such a straightforward analysis of ligand binding by surface-tethered aptamers as demonstrated here.

Importantly, specific analysis of dopamine by the aptamer-modified electrodes currently seems to be the simplest and most reliable of the hitherto suggested approaches (Table 2) as well as most applicable for direct analysis of dopamine levels in brain or brain tissues,³¹ once the stability of the aptamer linkage

to the electrode surface is increased (on conditions of either the same as demonstrated here or improved selectivity and sensitivity of analysis). SPR analysis with a dopamine receptor as a biorecognition unit³² suggests a reasonable alternative though not for *in vivo* applications, and recently the encouraging results have been obtained with modified Si nanoparticles³³ which fluorescence may be quenched by the oxidized dopamine molecules, through the Förster resonance energy transfer. In other sensing schemes, non-interfering NT species (dihydroxyphenylacetic acid, homovanillic acid, tyramine, and serotonin, see Table 2) should be either referred to NT metabolites or dopamine-unrelated NTs, which oxidation potentials are quite different from those of dopamine and other catecholamines.⁹ Thus, the possibility of specific analysis of dopamine by those assays,³⁴⁻³⁶ in the presence of structurally related NTs, remains unclear.

Table 2. Some analytical characteristics of the existing sensors for specific analysis of dopamine in the presence of other NTs and their metabolites

Electrode modification	LR (μM)	LOD (μM)	NT&NT metabolites	Detection method	ref
Au/DA-RC	0.0006-4.6	5.6×10^{-4}	DOPAC, DOPA	SPR	32
GCE/laccase/ /MWCNTs	1-30	0.4	DOPAC	CV, DPV	34
Au/MWCNTs/ /poly(AABA)	0.05-2	0.02	Tyr, HVA, DOPAC	CV, DPV, EQCM	35
HOPG	No data	No data	5-HT	CV	36
APTMS SiNPs	0.005-10	3×10^{-4}	NE, 5-HT	Fluorescence	33
Au/Cys/ /RNA aptamer	0.1-2 0.1-5	0.1	E, NE, DOPA, DOPAC, CH, Tyr, HMP	CV, CA	This work and 9

AABA-3: acrylamidophenylboronic acid; **APTMS SiNPs:** (3-aminopropyl) trimethoxysilane silicon nanoparticles; **Cys:** cysteamine; **CH:** catechol; **DA-RC-D₃:** dopamine receptor; **DOPA:** 3-(3,4-dihydroxyphenyl)-alanine; **DOPAC:** 3,4-dihydroxyphenylacetic acid; **E:** epinephrine; **HMP:** 4-hydroxy-4-methoxyphenethylamine hydrochloride; **5-HT:** serotonin; **HVA:** homovanillic acid; **NE:** norepinephrine; **Tyr:** tyramine; **LOD:** limit of detection; **LR:** linear range; **DPV:** differential pulse voltammetry; **EQCM:** electrochemical quartz crystal balance; **SPR:** surface plasmon resonance; **SWV:** square wave voltammetry;

Conclusions

The surface state/surface density of the dopamine RNA aptamer immobilized at the electrodes has been shown to dramatically affect the dopamine binding ability of the aptamer, being maximal for the RNA aptamer monolayer composed of the aptamer molecules lying “flat” on the electrode surface, but not for the maximal achievable aptamer surface coverages. Electrostatic regulation of the aptamer binding to the

cysteamine SAM-modified electrodes allowed the improvement of the RNA aptamer binding affinity for dopamine, with the dopamine-aptamer complex dissociation constant decreasing to 0.12 μM as compared to 1.6 μM shown in solution. 0.1-2 μM dopamine could be specifically and sensitively detected by the optimized aptamer-modified electrodes, with no interference from electrochemically/structurally related catecholamines, such as norepinephrine, L-DOPA, and catechol. The results strongly suggest that the surface state of the aptamer/its surface coverage should be considered as a critical parameter in the construction of the affinity biosensors, particularly in the case of aptamers which biorecognition reactions can be sterically hindered by a too dense population of the aptamer molecules at the electrode surface. These results should be taken into account in design and analysis of other aptamer-electrode systems in which an electrochemically inactive ligand does not allow direct correlation of the aptamer surface state and its binding affinity.

Acknowledgements

The work was supported by the Danish National Research Foundation (DNRF) through their support to the CDNA, grant number DNRF8. IÁM thanks the FICYT and the 7th WP of the European Union, Marie Curie Actions, for the post-doctoral grant ACA14-22.

Notes and references

- J.-M. Beaulieu and R. R. Gainetdinov, *Pharmacol. Rev.*, 2011, **63**, 182-217.
- A. Grace, *Neurosci.*, 1991, **41**, 1-24.
- J. A. Obeso, M. C. Rodriguez-Oroz, C. G. Goetz, C. Marin, J. H. Kordower, M. Rodriguez, E. C. Hirsch, M. Farrer, A. H. Schapira and G. Halliday, *Nat. Med.*, 2010, **16**, 653-661.
- D. Sulzer, *Neuron*, 2011, **69**, 628-649.
- S. E. Hyman and R. C. Malenka, *Nat. Rev. Neurosci.*, 2001, **2**, 695-703.
- A. Michael and L. Borland, in *Electrochemical Methods for Neuroscience*, eds. A.C. Michael and L.M. Borland, Boca Raton (FL), CRC Press, 2007. Chapter 2.
- J. Bicker, A. Fortuna, G. Alves and A. Falcão, *Anal. Chim. Acta*, 2013, **768**, 12-34.
- A. Pandikumar, G. T. Soon How, T. P. See, F. S. Omar, S. Jayabal, K. Z. Kamali, N. Yusoff, A. Jamil, R. Ramaraj, S. A. John, H. N. Lim and N. M. Huang, *RSC Advances*, 2014, **4**, 63296-63323.
- E. Farjami, R. Campos, J. Nielsen, K. Gothelf, J. Kjems and E. E. Ferapontova, *Anal. Chem.*, 2013, **85**, 121-128.
- N. Jia, Z. Wang, G. Yang, H. Shen and L. Zhu, *Electrochem. Commun.*, 2007, **9**, 233-238.
- S. B. A. Barros, A. Rahim, A. A. Tanaka, L. T. Arenas, R. Landers and Y. Gushikem, *Electrochim. Acta*, 2013, **87**, 140-147.
- R. L. McCreery, in *Voltammetric Methods in Brain Systems*, eds. A. A. Boulton, G. B. Baker and R. N. Adams, Humana Press, Totowa, NJ, 2010.
- K. Jackowska and P. Krysinski, *Anal. Bioanal. Chem.*, 2013, **405**, 3753-3771.

- 1
2
3
4
5
6
7
8
9
10
11
12
13
14
15
16
17
18
19
20
21
22
23
24
25
26
27
28
29
30
31
32
33
34
35
36
37
38
39
40
41
42
43
44
45
46
47
48
49
50
51
52
53
54
55
56
57
58
59
60
14. E. E. Ferapontova and K. V. Gothelf, *Curr. Org. Chem.*, 2011, **15**, 498-505.
 15. R. White, J. Liu, M. D. Morris, F. Macazo and L. Schoukroun-Barnes, *J. Electrochem. Soc.*, 2014, **161** (5) H301-H313.
 16. B. R. Baker, R. Y. Lai, M. S. Wood, E. H. Doctor, A. J. Heeger and K. W. Plaxco, *J. Am. Chem. Soc.*, 2006, **128**, 3138-3139.
 17. E. E. Ferapontova, E. M. Olsen and K. V. Gothelf, *J. Am. Chem. Soc.*, 2008, **130**, 4256-4258.
 18. S. V. Lemesenko, T. Powdrill, Y. Y. Belosludtsev and M. Hogan, *Nucl. Acids Res.*, 2001, **29**, 3051-3058.
 19. R. Campos and E. E. Ferapontova, *Electrochim. Acta*, 2014, **126**, 151-157.
 20. E. Farjami, R. Campos and E. E. Ferapontova, *Langmuir*, 2012, **28**, 16218-16226.
 21. C. Mannironi, A. DiNardo, P. Fruscoloni and G. P. Tocchini-Valentini, *Biochemistry*, 1997, **36**, 9726-9734.
 22. J. C. Hoogvliet, M. Dijkstra, B. Kamp and W. P. van Bennekom, *Anal. Chem.*, 2000, **72**, 2016-2021.
 23. G. Hartwich, D. J. Caruana, T. de Lumley-Woodyear, Y. Wu, C. N. Campbell and A. Heller, *J. Am. Chem. Soc.*, 1999, **121**, 10803-10812.
 24. D. Pastré, V. Joshi, P. A. Curmi and L. Hamon, *Small*, 2013, **9**, 3630-3638.
 25. A. Nabok, A. Tsargorodskaya, D. Gauthier, F. Davis, S. P. J. Higson, T. Berzina, L. Cristofolini and M. P. Fontana, *J. Phys. Chem. B*, 2009, **113**, 7897-7902.
 26. A. J. Bard and L. R. Faulkner, *Electrochemical methods: fundamentals and applications*, Wiley New York, 1980.
 27. R. H. Sarma, *Nucleic Acid Geometry and Dynamics*, Pergamon Press, New York, 1980.
 28. X. Zhang, M. R. Servos and J. Liu, *Langmuir*, 2012, **28**, 3896-3902.
 29. G. Scatchard, *Ann. N. Y. Acad. Sci.*, 1949, **51**, 660-672.
 30. M. Jarczewska, L. Kekedy-Nagy, J. S. Nielsen, R. Campos, J. Kjems, E. Malinowska and E. E. Ferapontova, *Analyst*, 2015, DOI: 10.1039/c1034an02354d.
 31. D. L. Robinson, A. Hermans, A. T. Seipel and R. M. Wightman, *Chem. Rev.*, 2008, **108**, 2554-2584.
 32. S. Kumbhat, D. R. Shankaran, S. J. Kim, K. V. Gobi, V. Joshi and N. Miura, *Biosens. Bioelectron.*, 2007, **23**, 421-427.
 33. X. Zhang, X. Chen, S. Kai, H. Y. Wang, J. Yang, F. G. Wu and Z. Chen, *Anal. Chem.*, 2015, **87**, 3360-3365.
 34. L. Xiang, Y. Lin, P. Yu, L. Su and L. Mao, *Electrochim. Acta*, 2007, **52**, 4144-4152.
 35. S. Hong, L. Y. S. Lee, M. H. So and K. Y. Wong, *Electroanalysis*, 2013, **25**, 1085-1094.
 36. A. N. Patel, S.-Y. Tan, T. S. Miller, J. V. Macpherson and P. R. Unwin, *Anal. Chem.*, 2013, **85**, 11755-11764.